

## Signatures of noise-enhanced stability in metastable states

A. Fiasconaro,<sup>1,\*</sup> B. Spagnolo,<sup>1</sup> and S. Boccaletti<sup>2</sup>

<sup>1</sup>*Dipartimento di Fisica e Tecnologie Relative and INFN-CNR, Group of Interdisciplinary Physics, Università di Palermo, Viale delle Scienze pad. 18, I-90128 Palermo, Italy*

<sup>2</sup>*Istituto dei Sistemi Complessi del CNR, Sezione di Firenze, Via Madonna del Piano, Sesto Fiorentino, Florence, Italy*

(Received 16 June 2005; revised manuscript received 13 September 2005; published 27 December 2005)

The lifetime of a metastable state in the transient dynamics of an overdamped Brownian particle is analyzed, both in terms of the mean first passage time and by means of the mean growth rate coefficient. Both quantities feature nonmonotonic behaviors as a function of the noise intensity, and are independent signatures of the noise enhanced stability effect. They can therefore be alternatively used to evaluate and estimate the presence of this phenomenon, which characterizes metastability in nonlinear physical systems.

DOI: [10.1103/PhysRevE.72.061110](https://doi.org/10.1103/PhysRevE.72.061110)

PACS number(s): 05.40.-a, 02.50.-r, 05.45.-a

### I. INTRODUCTION

Metastability is a generic feature of many nonlinear systems, and the problem of the lifetime of a metastable state involves fundamental aspects of nonequilibrium statistical mechanics [1]. Metastable states, indeed, have been proved to play a crucial role, e.g., in protein folding dynamics, Ising spin glasses, complex dynamics of large molecules at surfaces, enhancement of cellular memory, and in dynamics of cellular reactive oxygen species [2]. The problem of the lifetime of a metastable state has been addressed in a variety of areas, including first-order phase transitions, Josephson junctions, field theory, and chemical kinetics [3].

Recently, the investigation of nonlinear dynamics in the presence of external noisy sources led to the discovery of some resonancelike phenomena, among which we recall stochastic resonance [4], resonant activation [5], and noise enhanced stability (NES) [6–8]. All these phenomena are characterized by a nonmonotonic behavior of some quantity as a function of the forcing noise intensity or the driving frequency, which reflects a constructive and counterintuitive effect of the noise acting on the nonlinear system. In particular, several theoretical studies have shown that the average escape time from a metastable state in fluctuating and static potentials has a nonmonotonic behavior as a function of the noise intensity [8–13]. This resonancelike behavior, which contradicts the monotonic behavior predicted by Kramers theory [14,15], is called the NES phenomenon: the stability of metastable or unstable states can be enhanced by the noise and the average lifetime of the metastable state is larger than the deterministic decay time. Furthermore, if more realistic noise sources (such as colored noise with a finite correlation time) are considered, the value of the noise intensity at which the maximum of the average escape time occurs is even larger than that corresponding to the white noise case, meaning that the NES effect could be easy to measure experimentally, because of the finite time correlations involved in any realistic noisy sources [12].

When considering a Brownian particle in the presence of a metastable fluctuating potential, the NES effect is always

obtained [6,8], regardless of the unstable initial position of the particle. More precisely, two different dynamical regimes occur: one is characterized by a nonmonotonic behavior of the average escape time, as a function of noise intensity, and the other features a divergence of the mean escape time when the noise intensity tends to zero, implying that the Brownian particle remains trapped within the metastable state in the limit of small noise intensities. The description of the transition from one dynamical regime to the other is yet an open question.

In this paper we analyze in more detail the divergent dynamical regime, and suggest an approach for detecting the stability of metastable states, that is alternative to the mean-first-passage-time (MFPT) technique. In particular, we find a nonmonotonic behavior of the MFPT with a minimum and a maximum as a function of the noise intensity for initial positions of the Brownian particle close to the point  $x_c$  where the potential shape intersects the  $x$  axis (see the inset of Fig. 1). In this regime the standard deviation of the escape time has a divergent behavior for small noise intensity. This means that the average escape time, which is a quantitative measure of the average lifetime of the metastable state, has in fact some statistical limitations to fully describe the stability of metastable states.

To complement the analysis of the transient dynamics of metastable states, we then introduce a different approach, based on the evaluation of the mean growth rate coefficient  $\Lambda$  as a function of the noise intensity. The  $\Lambda$  coefficient is evaluated by the use of a procedure similar to that for the calculation of the Lyapunov exponent in stochastic systems, e.g., we consider the evolution of the separation  $\delta x(t)$  between two neighboring trajectories of the Brownian particle [16–19]. We will show that also the  $\Lambda$  coefficient displays a nonmonotonic behavior (with a clear minimum) as a function of the noise intensity, thus representing an independent way for detecting and estimating the NES effect. The paper is organized as follows. In the next section the divergent dynamical regime of the MFPT and its standard deviation are considered. In the third section we introduce a new physical quantity, that is the *mean growth rate coefficient*, which is useful to characterize the transient dynamics of metastable states. In the final section we draw the conclusions.

\*Email address: [afiasconaro@gip.dft.unipa.it](mailto:afiasconaro@gip.dft.unipa.it)

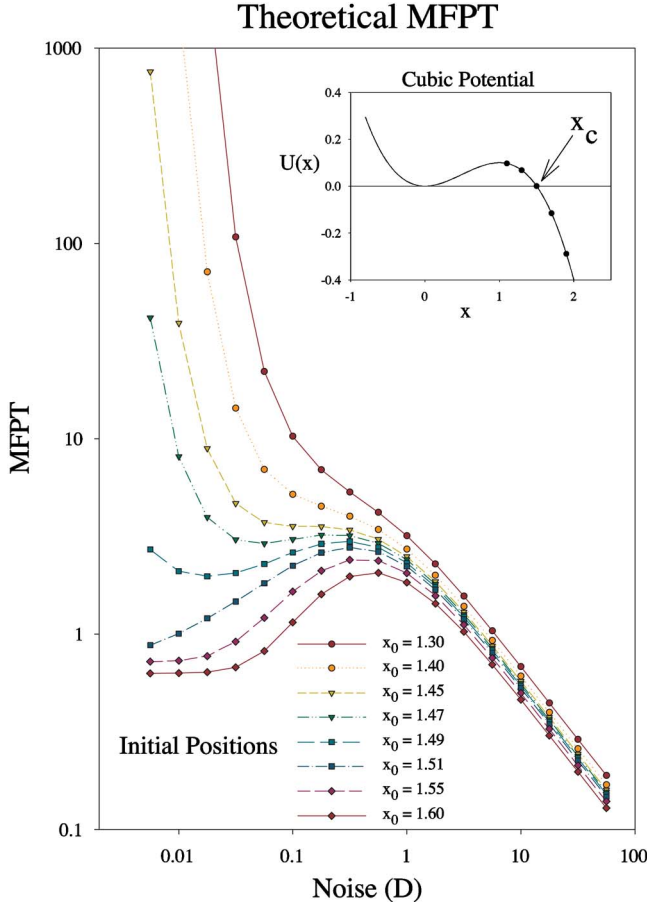


FIG. 1. (Color online) MFPT  $\tau(x_0, x_F)$  evaluated from expression (3) vs the noise intensity  $D$ , for  $x_F=2.2$  and for different initial positions  $x_0$  (see the legend). The NES effect is observed for  $x_0 > x_c$ , while the divergence regime corresponds to  $x_u < x_0 < x_c$ . Inset: the cubic potential  $U(x)$  with the metastable state at  $x=0$ . The arrow indicates the intersection point  $x_c=1.5$  between the potential curve and the horizontal axis.

## II. MEAN FIRST PASSAGE TIME

The starting point of our analysis is a Brownian particle in one spatial dimension, obeying the following Langevin equation:

$$\dot{x} = -\frac{dU(x)}{dx} + \sqrt{D}\xi(t), \quad (1)$$

where  $\xi(t)$  is a white Gaussian noise source with zero mean and  $\delta$  correlated in time [ $\langle \xi(t) \rangle = 0$  and  $\langle \xi(t)\xi(t+\tau) \rangle = \delta(\tau)$ ], and  $U(x)=0.3x^2-0.2x^3$  is a cubic potential, whose shape is shown in the inset of Fig. 1. The potential profile has a local stable state at  $x_s=0$ , an unstable state at  $x_u=1$ , and intersects the  $x$  axis at  $x_c=1.5$ .

After fixing a given target position  $x_F > x_c$ , the MFPT  $\tau(x_0, x_F)$  (the average time for a particle starting from an initial position  $x_0$  to reach  $x_F$ ) is given by the closed analytical expression [15,20]

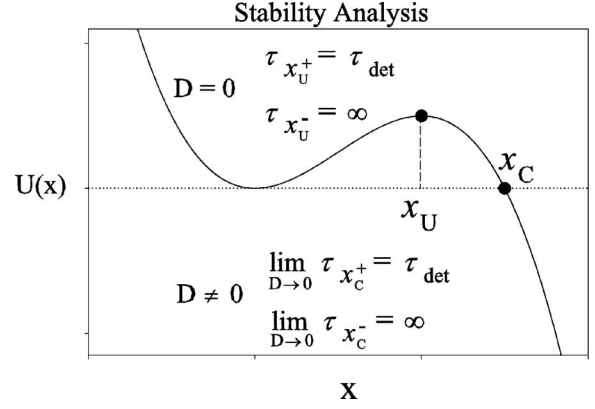


FIG. 2. Critical stability positions for noiseless and noisy statistics. In the first case ( $D=0$ ) a particle starting from the position  $x_0=x_u-\varepsilon$  has an escape time ( $\tau_{x_u^-}$ ) equal to infinity, and a particle starting from the position  $x_0=x_u+\varepsilon$  has an escape time equal to the deterministic one  $\tau_{x_c^+}=\tau_{det}$ . The same behavior is recognized in the second case ( $D \neq 0$ ) in the limit  $D \rightarrow 0$  for the critical position  $x_c$ . This means that the “unstable equilibrium” position in the stochastic case (from the point of view of the stability of the metastable state) is not  $x_0=x_u$ , but  $x_0=x_c$ .

$$\tau(x_0, x_F) = \frac{2}{D} \int_{x_0}^{x_F} e^{2u(z)} \int_{-\infty}^z e^{-2u(y)} dy dz, \quad (2)$$

where  $u(x)=U(x)/D$  is the dimensionless potential profile, obtained by normalizing  $U(x)$  to the noise intensity  $D$ . The double integral (2) can be evaluated (in part analytically, in part numerically), giving rise to

$$\tau(x_0, x_F) = \frac{2}{D} \int_{x_0}^{x_F} e^{2u(z)} G(z) dz, \quad (3)$$

where  $G(z)=0.6046e^{-z}[I_{-1/3}(z)+I_{1/3}(z)]-\frac{1}{2}{}_2F_2(\frac{1}{2}, 1; \frac{2}{3}, \frac{4}{3}; -2z)+\int_0^z e^{-2u(y)} dy$ ,  $z=1/(10D)$ ,  $I_n(z)$  is the modified Bessel function of the first kind, and  ${}_pF_q(a_1, a_2; b_1, b_2; z)$  is the generalized hypergeometric function.

In Fig. 1 the evaluation of expression (3) for  $x_F=2.2$  and for different initial positions  $x_0$  (as sketched in the legend) is reported. Two different regimes can be observed, depending on the initial state of the particle: (i) the NES effect for all initial conditions  $x_0 > x_c$ , and (ii) the divergent regime for  $x_u \leq x_0 < x_c$ , where  $x_u=1$  is the location of the relative maximum of the potential profile. The intersection point  $x_c$  corresponds to the unstable point  $x_u$ , in the limit  $D \rightarrow 0$ , with respect to the stability of the metastable state. In fact when the Brownian particle goes away from this point the average lifetime diverges for  $x_0 < x_c$  and it is equal to the deterministic escape time for  $x_0 \geq x_c$  (see Fig. 2).

In this latter regime, for all initial positions  $x_0$  smaller than (but sufficiently close to)  $x_c$ , the MFPT displays a non-monotonic behavior with a minimum and a maximum. For very low noise intensities, the Brownian particle is trapped into the potential well, as a consequence of the divergence of the MFPT in the limit  $D \rightarrow 0$ . For increasing noise intensity, the particle can escape out more easily, and the MFPT decreases. As the noise intensity reaches a value  $D \approx \Delta U=0.1$

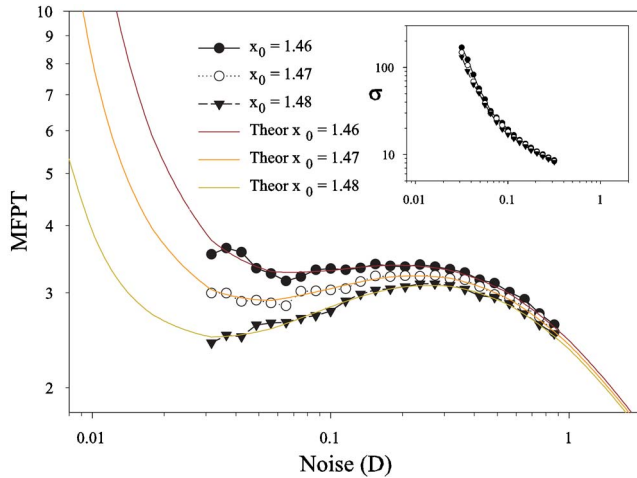


FIG. 3. (Color online) Numerical estimation of the MFPT (symbols) vs  $D$  for  $x_0=1.46$  (filled circles),  $x_0=1.47$  (empty circles), and  $x_0=1.48$  (filled triangles). The solid curves are the corresponding estimations of the MFPT from Eq. (3). Inset: standard deviation  $\sigma$  of MFPT's corresponding to different noise realizations vs  $D$  for the same initial positions  $x_0$ .

(corresponding to the potential barrier height), the concavity of the MFPT curves changes. Close to such a noise intensity, the escape process of the Brownian particle is slowed down, due to the fact that the probability to reenter the well is increased. At higher noise intensities, one recovers a monotonic decreasing behavior of the MFPT. In summary, from inspection of Fig. 1, the behavior of MFPT vs  $D$  goes with continuity from a monotonic divergent behavior to a non-monotonic finite behavior (typical NES effect), passing through a nonmonotonic divergent behavior with a minimum and a maximum.

In the following we will focus on this last dynamical regime. First of all, we compare the theoretical results of Fig. 1 with direct numerical simulations of Eq. (1). Namely, we numerically integrate Eq. (1) with different initial conditions  $x_0 \leq x_c$ . For each initial condition (and for each value of the noise intensity  $D$ ), the integration is performed over an ensemble of  $N_R=350\,000$  different realizations of the white noise process  $\xi(t)$ . The target position  $x_F=2.2$  is selected, and the MFPT (calculated as the ensemble average of the first passage times through  $x_F$  for different noise realizations) is reported in Fig. 3, together with the corresponding theoretical curves. The agreement between theoretical predictions and numerical simulations is very good. For low values of  $D$ , however, we cannot reproduce the theoretical curves because of the finiteness of the integration time ( $T_{max}=20\,000$  a.u.) and of the number of realizations. The MFPT evaluated in this range of noise intensities, therefore, tends to the deterministic escape time.

The numerical study of Eq. (1) allows us to also calculate the standard deviation  $\sigma$  of the set of first passage times obtained for different noise realizations. The results are shown in the inset of Fig. 3 for the same values of  $x_0$ , where a divergent behavior of  $\sigma(D)$  is visible in the limit  $D \rightarrow 0$ . Such a feature confirms that the only information on the MFPT is not sufficient to fully unravel the statistical proper-

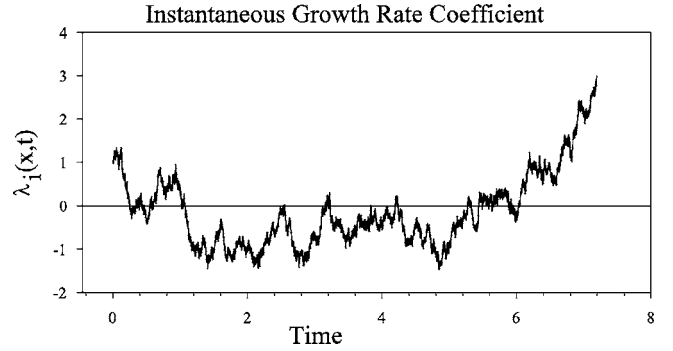


FIG. 4.  $\lambda_i(x,t)$  (see text for definition) vs time, for  $x_0=1.3$ ,  $x_F=3$ , and  $D=1$ .

ties of this dynamical regime, and motivated our search for a complementary approach.

### III. MEAN GROWTH RATE COEFFICIENT

This approach is done by monitoring the properties of the *mean growth rate coefficient*  $\Lambda$ . Let  $\delta x_0 = \delta x(t=0) \ll 1$  be the initial separation of two neighboring Brownian particles subjected to the same noise process  $\xi(t)$ . By linearization of Eq. (1), the evolution of the particle separation  $\delta x(t)$  is given by

$$\delta \dot{x}(t) = - \frac{d^2 U(x)}{dx^2} \delta x(t) = \lambda_i(x,t) \delta x(t), \quad (4)$$

and allows for the definition of an instantaneous growth rate  $\lambda_i(x,t)$ . It is important to stress that, in Eq. (4),  $d^2 U(x)/dx^2$  is calculated onto (and as so, it is a function of) the noisy trajectory  $x[\xi(t)]$  [21]. The growth rate coefficient  $\Lambda_i$  (for the  $i$ th noise realization), is then defined as the longtime average of the instantaneous  $\lambda_i$  coefficient over  $\tau(x_0, x_F)$  [16–19]

$$\Lambda_i = \frac{1}{\tau(x_0, x_F)} \int_0^{\tau(x_0, x_F)} \lambda_i(x,s) ds. \quad (5)$$

Notice that, in the limit  $\tau(x_0, x_F) \rightarrow \infty$ , Eq. (5) coincides formally with the definition of the maximum Lyapunov exponent, and that, therefore, our  $\Lambda_i$  coefficient has the meaning of a finite-time Lyapunov exponent, since we are interesting in characterizing a transient dynamics. The mean growth rate coefficient (MGRC)  $\Lambda$  is then obtained by ensemble averaging the  $\Lambda_i$  coefficients over the  $N_R$  different noise realizations ( $\Lambda = \sum \Lambda_i / N_R$ ).

In our simulations of Eq. (4), an integration time step of  $dt=0.0001$ , and an initial condition  $\delta x_0=0.01$  are used. The instantaneous growth rate  $\lambda_i(x,t)$  is calculated over  $N_T$  small subintervals of the trajectory, each of them corresponding to a time interval  $\tau=5dt$ .

In Fig. 4 we report the behavior of  $\lambda_i(x,t)$  as a function of time for  $D=1$ . The  $\lambda_i(x,t)$  coefficient is negative for most of the time, due to noise-induced local stability of metastable state. As the Brownian particle reaches the point at which the potential changes its concavity,  $\lambda_i(x,t)$  becomes positive. As for the  $\Lambda$  coefficient, fixing  $x_F=20$ , it displays a nonmonotonic behavior with a minimum as a function of noise inten-

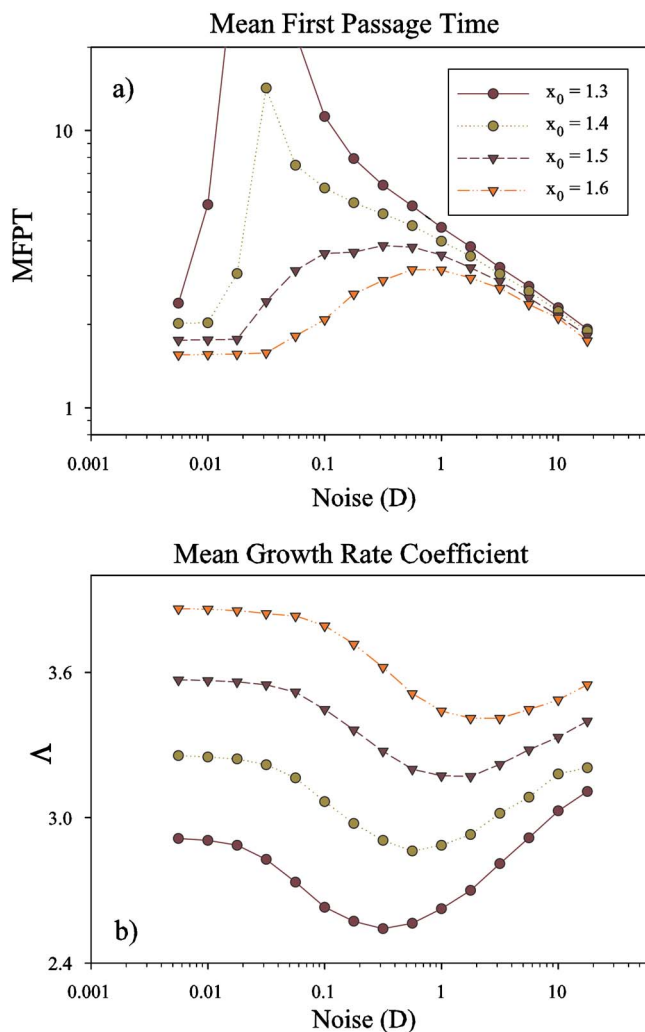


FIG. 5. (Color online) (a) Numerical estimation of the MFPT for various initial positions (as in the legend) and (b) the corresponding MGRC vs the noise intensity  $D$ . The average has been performed over 20 000 realizations. The absorbing boundary is  $x_F=20$ , and the maximum waiting time used in the simulations is  $T_{max}=20\,000$ .

sity [see Fig. 5(b)], though being always positive. This reflects the fact that the Brownian particles always escape in average from the metastable state, but the nonmonotonic behavior of the MGRC marks the presence of the NES effect. In particular, the closer the initial positions of the particles are to  $x_0$ , the smaller the MGRC. Notice that  $\lambda_i(x, t)$  is proportional to the trajectory of the Brownian particle because the potential is a cubic one. Any metastable state, however, can be described through a local cubic potential even if the real potential has other local or global stable states.

Figure 5 is a comparative plot of the numerically calculated MFPT (a) and the corresponding MGRC (b) vs  $D$  for various initial positions of the Brownian particles. The MFPT's plot [Fig. 5(a)] shows the divergent behavior as a maximum, which is shifted towards lower values of the noise intensity. Because of the finiteness of the ensemble of particles considered in our numerical experiments, observation of the divergence in time is prevented in our simulations, and for very low noise intensities ( $D \rightarrow 0$ ) the deterministic es-

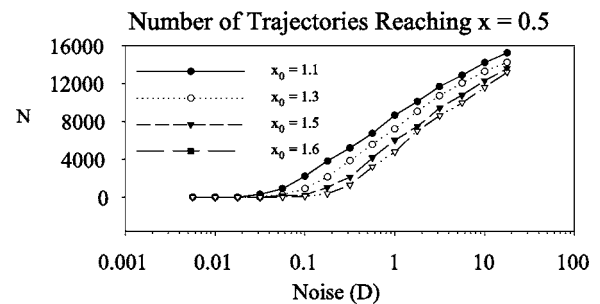


FIG. 6. Number of trajectories reaching the position  $x=0.5$  inside the potential well. In this position the instantaneous growth rate  $\lambda_i(x, t)$  is equal to zero.

cape time is retrieved. The trajectories of the Brownian particles trapped into the potential well in the limit of  $D \rightarrow 0$  lead to the singularity of the MFPT observed in theoretical evaluation of Fig. 1. However, the observation time in a digital simulation is finite and for some value of noise intensity it becomes smaller than the average escape time of a particle trapped in the well. Therefore, the simulated escape time has a maximum at this point. Besides, the ensemble of particles in a numerical experiment is also finite. So for  $D \rightarrow 0$ , when the probability for a particle to be trapped in the well decreases exponentially to zero, we do not observe such particles in simulations and the MFPT tends to the deterministic escape time at  $D \rightarrow 0$  [see Fig. 5(a)] [11].

As can be seen in Fig. 5(b), the maximum of the MFPT curve is reflected by a local minimum in the MGRC shape, which is, however, slightly shifted towards lower values of the noise intensity. This is because, at low noise intensities, not all the particles coming back into the potential well reach positions around the metastable state with positive concavity, which instead will be attained by particles experiencing larger noise kicks. These latter ones contribute to lower the value of  $\Lambda$ , due to the negative contributions of the  $\lambda_i$ 's corresponding to such positions (see Fig. 4).

We note that the behavior of the MGRC as a function of the noise intensity is strongly affected by the characteristic potential shape of a metastable state. In order to clarify the behavior of MGRC in the limit of  $D \rightarrow 0$  we report in Fig. 6 the number  $N$  of the Brownian particles that reach the position  $x=0.5$  as a function of the noise intensity. This is the flex point of the potential where the instantaneous growth rate  $\lambda_i(x, t)$  is equal to zero. We see that for low noise intensities this number goes to zero, producing an increasing behavior of the MGRC [see Fig. 5(b)].

#### IV. CONCLUSIONS

It is worthwhile to note that the divergence of standard deviation of MFPT when  $D \rightarrow 0$  corresponds to a big tail in the first passage time distribution (see Refs. [8,10], where this point is explained in detail). This means that the temporary trapping of the particle into the potential well is a rare event, which strongly affects the average lifetime of the metastable state. As a consequence the value of MFPT increases with decreasing noise intensities, giving rise to a

more pronounced maximum [see Fig. 5(b)]. Moreover, temporary trapped particles have trajectories like that shown in Fig. 4. The time interval in which the  $\lambda_i$  coefficient is negative is longer for decreasing noise intensities. This produces a more pronounced minimum in the MGRC. For smaller noise intensities the number of trajectories for which the particle enters into the well decreases and therefore the MGRC increases, reaching the deterministic value [see Figs. 5(b) and 6].

In conclusion, we investigated the average escape time from a metastable state in a cubic potential profile for different initial unstable positions of the Brownian particles. The

two introduced measures (the behavior of the MFPT and of the MGRC) furnish suitable tools to detect the lifetime of metastable states in the presence of external noise, and, as so, they can be alternatively used in many relevant circumstances, such as understanding activation processes in complex systems characterized by energy landscape [2].

#### ACKNOWLEDGMENTS

This work was supported by MIUR, MIUR-FIRB, and INFN-CNR.

- 
- [1] G. Parisi, *Nature* **433**, 221 (2005); S. Kraut and C. Grebogi, *Phys. Rev. Lett.* **93**, 250603 (2004); M. I. Dykman and D. Ryvkine, *ibid.* **94**, 070602 (2005); H. Larralde and F. Leyvraz, *ibid.* **94**, 160201 (2005).
- [2] C. M. Dobson, *Nature* **426**, 884 (2003); A. Cavagna, I. Giardinina, and G. Parisi, *Phys. Rev. Lett.* **92**, 120603 (2004); R. Otero *et al.*, *Nat. Mater.* **3**, 779 (2004); M. Acar, A. Becskei, and A. van Oudenaarden, *Nature* **435**, 228 (2005); C. Lee *et al.*, *Nat. Rev. Mol. Cell Biol.* **5**, 7 (2004).
- [3] M. Chandran, R. T. Scalettar, and G. T. Zimányi, *Phys. Rev. Lett.* **89**, 187001 (2002); O. A. Tretiakov, T. Gramespacher, and K. A. Matveev, *Phys. Rev. B* **67**, 073303 (2003); A. J. Berkley, H. Xu, M. A. Gobrod, R. C. Ramos, J. R. Anderson, C. J. Lobb, and F. C. Wellstood, *ibid.* **68**, 060502(R) (2003); A. L. Pankratov and B. Spagnolo, *Phys. Rev. Lett.* **93**, 177001 (2004); H. Larralde and F. Leyvraz, *ibid.* **94**, 160201 (2005).
- [4] L. Gammaitoni, F. Marchesoni, and S. Santucci, *Rev. Mod. Phys.* **70**, 223 (1998); V. S. Anishchenko *et al.*, *Phys. Usp.* **42**, 7 (1999); R. N. Mantegna, B. Spagnolo, and M. Trapanese, *Phys. Rev. E* **63**, 011101 (2001); T. Wellens, V. Shatokhin, and A. Buchleitner, *Rep. Prog. Phys.* **67**, 45 (2004).
- [5] C. R. Doering and J. C. Gadoua, *Phys. Rev. Lett.* **69**, 2318 (1992); M. Marchi *et al.*, *Phys. Rev. E* **54**, 3479 (1996); R. N. Mantegna and B. Spagnolo, *Phys. Rev. Lett.* **84**, 3025 (2000).
- [6] R. N. Mantegna and B. Spagnolo, *Phys. Rev. Lett.* **76**, 563 (1996).
- [7] J. E. Hirsch, B. A. Huberman, and D. J. Scalapino, *Phys. Rev. A* **25**, 519 (1982); I. Dayan, M. Gitterman, and G. H. Weiss, *Phys. Rev. A* **46**, 757 (1992); F. Apostolico, L. Gammaitoni, F. Marchesoni, and S. Santucci, *Phys. Rev. E* **55**, 36 (1997).
- [8] N. V. Agudov and B. Spagnolo, *Phys. Rev. E* **64**, 035102(R) (2001).
- [9] A. A. Dubkov, N. V. Agudov, and B. Spagnolo, *Phys. Rev. E* **69**, 061103 (2004).
- [10] A. Fiasconaro, D. Valenti, and B. Spagnolo, *Physica A* **325**, 136 (2003).
- [11] N. V. Agudov, R. Mannella, A. V. Safonov, and B. Spagnolo, *J. Phys. A* **37**, 5279 (2004).
- [12] A. Fiasconaro, D. Valenti, and B. Spagnolo, *Modern Problems of Statistical Physics* **2**, 101 (2003) (<http://www.mptalam.org/>).
- [13] N. V. Agudov and A. N. Malakhov, *Phys. Rev. E* **60**, 6333 (1999); D. Dan, M. C. Mahato, and A. M. Jayannavar, *ibid.* **60**, 6421 (1999); R. Wackerbauer, *ibid.* **59**, 2872 (1999); A. Mielke, *ibid.* **84**, 818 (2000).
- [14] H. A. Kramers, *Physica (Amsterdam)* **7**, 284 (1940).
- [15] P. Hänggi, P. Talkner, and M. Borkovec, *Rev. Mod. Phys.* **62**, 251 (1990).
- [16] W. Ebeling, H. Herzel, W. Richert, and L. Schimansky-Geir, *Z. Angew. Math. Mech.* **66**, 141 (1986); L. Schimansky-Geir and H. Herzel, *J. Stat. Phys.* **70**, 141 (1993).
- [17] G. Paladin, M. Serva, and A. Vulpiani, *Phys. Rev. Lett.* **74**, 66 (1995); V. Loreto, G. Paladin, and A. Vulpiani, *Phys. Rev. E* **53**, 2087 (1996).
- [18] G. Boffetta, M. Cencini, M. Falcioni, and A. Vulpiani, *Phys. Rep.* **356**, 367 (2002).
- [19] A. Witt, A. Neiman, and J. Kurths, *Phys. Rev. E* **55**, 5050 (1997).
- [20] C. W. Gardiner, *Handbook of Stochastic Methods*, 2nd ed. (Springer-Verlag, Berlin, 1994).
- [21] In our simplified example  $\lambda_i = -d^2U(x)/dx^2 = 1.2x(t) - 0.6$ .